

Prospects of neutrino oscillation measurements in the detection of reactor antineutrinos with a medium-baseline experiment

Mikhail Batygov,^{1,*} Stephen Dye,^{1,†} John Learned,^{1,‡}
Shigenobu Matsuno,^{1,§} Sandip Pakvasa,^{1,¶} and Gary Varner^{1,**}

¹*Department of Physics and Astronomy, University of Hawaii at Manoa, Honolulu, Hawaii 96822, USA*

Despite the dramatic progress made in neutrino oscillation studies recently, several fundamental neutrino parameters remain either unknown or poorly measured. We discuss in detail a method for their measurement by precision studies of oscillation-caused neutrino energy spectrum distortions, for which a large underwater inverse beta decay detector appears to be a perfect tool. Results determine optimal baselines and necessary exposures in the presence of systematic uncertainties and the unavoidable background from terrestrial antineutrinos.

PACS numbers: 14.60.Pq, 26.65.+t, 28.50.Hw

INTRODUCTION

Neutrino flavor transformations are determined by the elements of the PMNS matrix [1, 2] and the differences between the squares of neutrino mass eigenvalues. PMNS matrix represents the mixture between flavor and mass eigenstates of neutrinos and is conventionally decomposed as shown in (1). Neutrino oscillation experiments can yield the best estimations for some of those parameters, which has been demonstrated by SNO [3] and KamLAND [4].

$$\begin{aligned}
 U &= \begin{bmatrix} U_{e1} & U_{e2} & U_{e3} \\ U_{\mu1} & U_{\mu2} & U_{\mu3} \\ U_{\tau1} & U_{\tau2} & U_{\tau3} \end{bmatrix} \\
 &= \begin{bmatrix} 1 & 0 & 0 \\ 0 & c_{23} & s_{23} \\ 0 & -s_{23} & c_{23} \end{bmatrix} \begin{bmatrix} c_{13} & 0 & s_{13}e^{-i\delta} \\ 0 & 1 & 0 \\ -s_{13}e^{i\delta} & 0 & c_{13} \end{bmatrix} \\
 &\times \begin{bmatrix} c_{12} & s_{12} & 0 \\ -s_{12} & c_{12} & 0 \\ 0 & 0 & 1 \end{bmatrix} \begin{bmatrix} e^{i\alpha_1/2} & 0 & 0 \\ 0 & e^{i\alpha_2/2} & 0 \\ 0 & 0 & 1 \end{bmatrix}, \tag{1}
 \end{aligned}$$

where $s_{ij} = \sin\theta_{ij}$, $c_{ij} = \cos\theta_{ij}$, δ is the phase factor (non-zero if neutrino oscillation violates CP symmetry), α_1 and α_2 Majorana phase factors (non-zero only if neutrinos are Majorana particles), to which neutrino oscillation experiments are not sensitive.

Besides the PMNS matrix, neutrino oscillations depend on mass eigenvalues or, more precisely, on the difference between the squared mass eigenvalues. If there are three neutrino mass eigenvalues, then there are only two independent differences, the third being either a sum or a difference of the other two.

Neutrinos studied in experiments are produced in certain flavor eigenstates with known abundances of each of them or, as an important special case, in only one flavor eigenstate. For example, neutrinos are generated in the atmosphere with the known $(\nu_\mu + \bar{\nu}_\mu)/(\nu_e + \bar{\nu}_e)$ ratio of about two for low energies; solar neutrinos and reactor antineutrinos are, initially, all ν_e and $\bar{\nu}_e$, respectively.

Detector sensitivity is, generally, flavor dependent. In particular, the inverse beta decay, the primary method for detecting reactor antineutrinos since the very beginning of neutrino experiments [5], involves electron antineutrinos only. Therefore, the number of detected neutrino events can be different from the no-oscillation expectation. The deficit of observed neutrinos compared to no-oscillation prediction was first detected in a solar neutrino experiment [6]. However the rate information alone could not provide sufficient evidence to ascribe conclusively the phenomenon of neutrino “disappearance” to flavor oscillations.

The energy dependence of neutrino oscillations not only changes the neutrino event rate but also distorts the observed neutrino energy spectrum. The spectrum distortion provides more information about the PMNS matrix components and neutrino mass eigenstates than rate studies alone can.

The inverse beta decay method offers excellent energy sensitivity, which is very valuable for the oscillation studies. Recoil smearing present in this reaction is small compared to detector energy resolution, the latter being the main limiting factor in the accuracy of $\bar{\nu}_e$ energy measurement. Other advantages include a relatively large cross section of the reaction and, most importantly, very powerful background suppression due to the characteristic double-coincidence signature. The limitations of this method are the $\bar{\nu}_e$ energy threshold of about 1.8 MeV and weak directionality.

The success of a neutrino oscillation experiment depends not only on the characteristics of the detector and on the neutrino source but also on the proper choice of the distance between the two (the baseline). There is no single baseline optimal for all neutrino oscillation studies. For example, the average baseline of KamLAND experiment, about 180 km, is fairly good for θ_{12} and especially for Δm_{12}^2 but not for θ_{13} , Δm_{13}^2 and Δm_{23}^2 . Moreover, such parameters as detector resolution, the amount, the nature of the background and the a-priori information about its properties can affect the optimal baseline value. A tunable baseline experiment, which implies movable detector or source, may have a big advantage here.

These considerations, along with the interest in studying terrestrial antineutrinos, led to the idea of a big KamLAND-like underwater detector [7, 8]. The potential of such a detector for neutrino oscillation parameter measurements was the primary motivation for the study presented here. However, the scope of the actual study is much wider and not limited to the Hanohano project. The results are in fact applicable to any similar medium-baselined experiment.

SPECTRUM DISTORTIONS DUE TO OSCILLATIONS

For baselines associated with current and near-future reactor based neutrino experiments (up to hundreds of kilometers), the matter effects [9, 10] critical in solar neutrino studies are not significant, so the vacuum oscillation approximation can be used. As was mentioned above, the inverse beta decay detection is sensitive to electron antineutrinos only. Reactors produce exclusively electron antineutrinos as well, so the observable effect is the apparent “disappearance” of a fraction of reactor-produced electron antineutrinos. The $\bar{\nu}_e$ “survival” probability is given by the formula [11, 12]:

$$\begin{aligned}
 P(\bar{\nu}_e \rightarrow \bar{\nu}_e) = 1 & - \cos^4(\theta_{13}) \sin^2(2\theta_{12}) \sin^2 \Delta_{12} \\
 & + \sin^2(2\theta_{13}) \cos^2(\theta_{12}) \sin^2 \Delta_{13} \\
 & + \sin^2(2\theta_{13}) \sin^2(\theta_{12}) \sin^2 \Delta_{23},
 \end{aligned} \tag{2}$$

where $\Delta_{ij} = \frac{|\Delta m_{ij}^2|R}{4E_\nu}$. Note that “atmospheric” mixing angle θ_{23} does not affect the ν_e survival and hence not measurable in electron neutrino disappearance experiments. Here, R is the “baseline”, the distance between the $\bar{\nu}_e$ source and the detector.

Given the evidence from solar neutrino experiments [13, 14] that $m_2 > m_1$, and the knowledge that $\Delta m_{23}^2 \gg \Delta m_{12}^2$ from SuperK [15], K2K [16], MINOS [17] on the one hand and KamLAND [4] on the other, only two neutrino hierarchies out of possible six are allowed with currently available data. They are commonly referred to as “Normal Hierarchy, NH” ($m_1 < m_2 < m_3$) and “Inverted Hierarchy, IH” ($m_3 < m_1 < m_2$) (Fig. 1). The former implies that $\Delta m_{13}^2 > \Delta m_{23}^2$, the latter that $\Delta m_{23}^2 > \Delta m_{13}^2$, so the sufficiently precise measurement of the those squared mass differences should be enough to establish the neutrino mass hierarchy.

The measurement of Δm_{13}^2 , Δm_{23}^2 and the mass hierarchy with this approach is possible, in theory, only if θ_{13} is finite and, in practice, if this mixing angle is large enough. Moreover, if the “solar” mixing is maximum ($\theta_{12} = \pi/4$), the Δm_{13}^2 and Δm_{23}^2 become mutually indistinguishable, thus still ruling out the mass hierarchy study, although their values may still be determined without knowing “which is which”. This maximum mixing is strongly disfavored by KamLAND [4] and essentially excluded by solar experiments [13, 14]. Unfortunately, the same can not be said about the θ_{13} since only the upper limit for this value exists today and there is no experimental evidence that it is not zero. If it is, then future $\bar{\nu}_e$ vacuum oscillation experiments are limited to probing θ_{12} and Δm_{12}^2 along with setting still better upper limits on the θ_{13} itself. That said, global analysis shows a slight preference for non-zero θ_{13} [18].

A typical reactor $\bar{\nu}_e$ spectrum [19, 20] multiplied by the inverse beta decay cross section [21] is shown in Figure 2, dotted. The antineutrinos are generated in β^- decays of short living fission products of initial fissionable fuel isotopes: ^{235}U , ^{238}U , ^{239}Pu , ^{241}Pu . For this study, the ratio of the isotopes is taken the same as in [4]. Such a spectrum can be observed at very short-baselined experiments (baseline $\ll 1$ km), where oscillation effects are negligible.

At much longer baselines (30 km and above), the “solar” oscillations governed by θ_{12} and Δm_{12}^2 lead to an energy-dependent deficit of the observed $\bar{\nu}_e$ events. The effect of those oscillations alone is the “coarse” oscillatory pattern

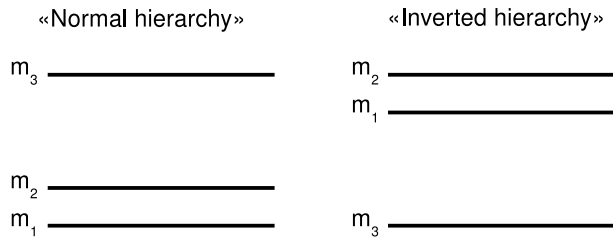


FIG. 1: Two neutrino mass hierarchies allowable with currently available data; all three combinations with $m_2 < m_1$ are excluded by solar experiments; the $m_1 < m_3 < m_2$ order is excluded by the fact that $\Delta m_{12}^2 \ll \Delta m_{23}^2 \approx \Delta m_{13}^2$.

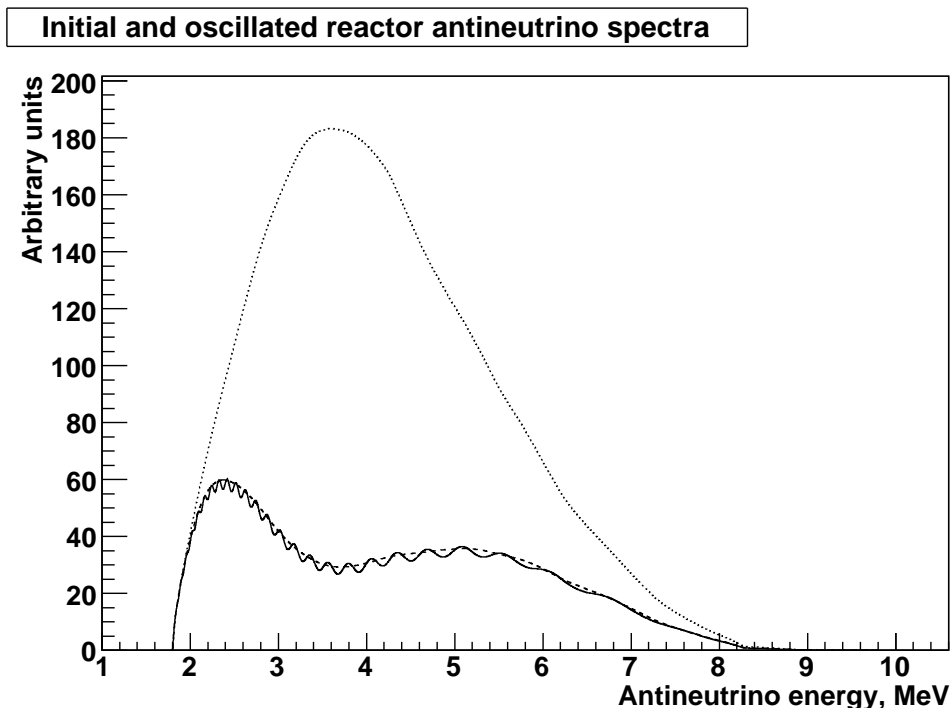


FIG. 2: Typical reactor $\bar{\nu}_e$ spectrum: non-oscillated (dotted), with $\theta_{13} = 0$ (dashed), and with $\theta_{13} = 0.05$ (solid).

of event deficit over the spectrum (Figure 2, dashed) with a high amplitude (determined by $\sin^2 2\theta_{12}$) and a relatively low frequency (determined by Δm_{12}^2).

The amplitude of oscillations driven by the squared mass differences Δm_{13}^2 and Δm_{23}^2 is proportional to $\sin^2 2\theta_{13}$ and much smaller than that of “solar” oscillations for any currently allowed value of this mixing angle. Because Δm_{13}^2 and Δm_{23}^2 are known to be larger than Δm_{12}^2 , the frequency of those sub-dominant oscillations is higher. A typical $\bar{\nu}_e$ energy spectrum expected for a non-zero θ_{13} is shown in Figure 2, solid.

The spectrum analysis approach has already been successfully used by KamLAND to set by now the best limits on Δm_{12}^2 and to confirm SNO and SuperK values for θ_{12} . The idea to measure the remaining three of the five oscillation parameters by precision measurement of the sub-dominant oscillation pattern in a reactor $\bar{\nu}_e$ disappearance experiment has been already suggested and thoroughly examined [22, 23, 24].

In this paper, we examine the capacity of an intermediate baseline (30-90 km) reactor $\bar{\nu}_e$ experiment for measuring θ_{12} , θ_{13} , Δm_{12}^2 , Δm_{13}^2 , Δm_{23}^2 and neutrino mass hierarchy. Although this study has been motivated by the project of a big underwater detector Hanohano ([7, 8]), we make no assertions specific for that particular choice. A special emphasis is placed on the systematic uncertainties and technical limitations present in any real experiment. In our

study of the sensitivity to each of the oscillation parameters we take into account the impact of those uncertainties, as well as some detector parameters and the baselines on the resulting performance to formulate in a quantitative way the requirements to which such an experiment must conform.

THE SCOPE OF ANALYSIS

In this study, we consider the measurement of all the oscillation parameters to which such $\bar{\nu}_e$ disappearance experiments are sensitive: θ_{12} , θ_{13} , Δm_{12}^2 , Δm_{13}^2 , Δm_{23}^2 . Three types of detector-related systematic uncertainties are considered which are present to some extent in any experiment and are capable of a non-trivial impact on the sensitivity to the target parameters. Although the success of the Borexino experiment [25] suggests that careful detector design can make the inverse-beta based $\bar{\nu}_e$ detection almost background-free, geologically produced antineutrinos [4, 26] will technically remain a background source for a reactor $\bar{\nu}_e$ study in the lower energy region. What makes this background especially significant is the lack of exact information about its overall intensity and the relative amounts of antineutrinos produced in the “Uranium-Radium” and “Thorium” decay series. This amounts to two more systematic uncertainties which have to be left unconstrained within geologically feasible models.

The following detector-related uncertainties were accounted for:

- The uncertainty in the predicted event rate. It is sensitive to the number of target protons (due to fiducial volume estimation error and uncertainty of the scintillator composition), the efficiency of coincidence selection cuts, and live time estimation error. For current similar experiments, this error tends to be on the order of 1 to 5%. Below we refer to this as “efficiency” error.
- The uncertainty in the detector energy resolution estimation. Although often ignored in current experiments, it can have a considerable effect on the measurement of the θ_{13} mixing angle from medium baselines. Numerically, it can be quite big (about 10%) depending on the detector calibration options.
- The “linear” energy scale uncertainty. This is the uncertainty in the average number of photoelectrons produced by an 1 MeV event. The amount of this uncertainty depends on the detector calibration as well. Normally it can be made quite small (around 1%) but its impact on the resulting accuracy of the parameter estimation may still be noticeable.

The energy scale in scintillator-based detectors is in fact substantially non-linear, this non-linearity always producing additional systematic uncertainties which are often rather tricky to parametrize. However the study of this error is very detector-specific, requires extensive Monte-Carlo simulations with real calibration data feedback and considering it at this stage would be too speculative. Although, KamLAND internal studies indicate that the nonlinear energy scale uncertainty is less of an issue than the linear one which we can take into account now, Hanohano or any other future experiment will have to revisit this issue, once the real experimental feedback from the detector becomes available.

The geo-neutrinos yield two more systematic uncertainties:

- Total detectable terrestrial antineutrino flux, conventionally expressed in Terrestrial Neutrino Units (TNU) defined as the number of inverse-beta decay interactions per 10^{32} free protons per year.
- The ratio of $\bar{\nu}_e$ originating from the ^{238}U decay chain to those coming from the ^{232}Th decay chain.

Although geological models do provide some guidelines for the expected geo-neutrino flux and KamLAND was able to produce the first experimental measurement of the flux, these data are of little use for the purpose of future experiments, including Hanohano, because the geo-neutrino estimation precision needed to produce an appreciable advantage over the “agnostic” approach is about one order of magnitude higher than available now.

STATISTICAL ANALYSIS PROCEDURE

Since we’ve included background and systematics in the analysis, the direct likelihood approach has been chosen over the combination of the matched digital filter and the Fourier transform of the spectrum employed in the earlier publications dedicated to or motivated by Hanohano project [8, 27]. This approach facilitates the accommodation of the systematic uncertainties and the background. The likelihood method used here is the unbinned statistical analysis similar to the one employed by KamLAND experiment [4, 26, 28, 29]. Instead of the real experimental data, a series of

“experiments” can be simulated as sequences of “events” with energies distributed according to the spectra distorted by different oscillation parameters (including the background). The potential sensitivity is essentially the ability of the data analysis to distinguish between different hypotheses about the oscillation parameter sets.

This study is based on the “rate+shape” likelihood function defined for a real or simulated experiment as:

$$L(\vec{E}_{\bar{\nu}_e}|\vec{\eta}) = e^{-N_{exp}} \prod_{i=1}^{N_{events}} f(E_{\bar{\nu}_e}^i|\vec{\eta}), \quad (3)$$

where $\vec{E}_{\bar{\nu}_e} = \{E_{\bar{\nu}_e}^1 \dots E_{\bar{\nu}_e}^N\}$ are the event energies, N — the number of observed events, $N_{exp}(\vec{\eta})$ — the expected number of events (given the set of parameters $\vec{\eta} \equiv \{\Delta m_{12}^2, \Delta m_{13}^2, \Delta m_{23}^2, \theta_{12}, \theta_{13}\}$), $f(E_{\bar{\nu}_e}^i|\vec{\eta})$ — $\bar{\nu}_e$ energy spectrum normalized to N_{exp} (after the distortion by the set of parameters $\vec{\eta}$). Note that while both $\vec{E}_{\bar{\nu}_e}$ and $\vec{\eta}$ are denoted as vectors, these vectors are in different spaces. The $\vec{E}_{\bar{\nu}_e}$ has as many dimensions as the sum of the number of $\bar{\nu}_e$ and background events in the experiment, and is fixed for a given experiment. The $\vec{\eta}$ lies in the parameter space, its dimensionality being the number of unknown parameters to be fitted, and is variable.

The best fit is obtained by varying the parameter vector $\vec{\eta}$ to achieve the maximum value of L or its logarithm, the latter often being more convenient to calculate and handle. After the best fit point $\vec{\eta}^0$ has been found, the general prescription to evaluate the sensitivity to some individual parameter η_k is the following:

- Make a small increment (or decrement) ϵ to the η_k from the “best fit” point η_k^0 : $\eta_k' = \eta_k^0 + \epsilon$.
- Find a new point of maximum likelihood by varying all the parameters $\vec{\eta}$ except for η_k which is kept fixed at η_k' . The new maximum L' over the subspace constrained by the requirement $\eta_k = \eta_k'$ is not higher than the global maximum L^0 .
- Repeat the above steps with varying ϵ until the condition $\log L^0 - \log L' = Q_{CL}$ is met for both positive and negative increments of ϵ . The corresponding points η_k^{low} and η_k^{high} will limit the confidence range for the k -th parameter.

The value Q_{CL} depends on the confidence level for which the range is to be determined. For an individual parameter variation and the confidence level equal to 1σ , $Q_1 = \frac{1}{2}$. In general, for a CL of $n\sigma$, $Q_n = \frac{1}{2}n^2$. When instead of a one-dimensional confidence range, a multidimensional confidence region in the parameter subspace is required, the values Q_{CL} will be different but the general procedure will not change. The same is true for the case of discriminating two discrete hypotheses, e.g. between the normal and the inverted neutrino mass hierarchies. More detailed information on the likelihood analysis can be found in [31].

For a simulated experiment, the experimental points $\vec{E}_{\bar{\nu}_e}$ do not exist in the first place and are generated according to some reasonable choice of parameters $\vec{\eta}$. Except for this initial stage, the rest of the analysis is the same as described above. If the initial choice of the parameters to simulate the events is not too far off, this procedure will yield an accurate prediction for the sensitivity of the actual experiment.

Systematic uncertainties are introduced by adding “hidden” parameters to the parameter space and allowing them to vary during the search for the maximum likelihood as well. When some information about these values is available a “penalty” term is subtracted from $\log(L)$ to account for the fact that big deviations from the central values of those hidden parameters are unlikely. If the parameters of uncertainty are normally distributed around their central value and if all systematic uncertainty parameters are uncorrelated, the “penalty” term takes on the form:

$$\frac{1}{2} \sum_{j=1}^{N_{SP}} \frac{\delta\eta_{k_j}^2}{\sigma_j^2}, \quad (4)$$

where N_{SP} is the number of systematic uncertainty parameters, k_j is the index of the parameter corresponding to the j -th uncertainty, $\delta\eta_{k_j}$ is the deviation of the k_j -th parameter from its most probable value, and σ_j is the value of systematic error ascribed to the j -th uncertainty. When some uncertainties are correlated, the penalty term becomes a more general positive definite quadratic form but for our current study that is not the case.

The full equation for the likelihood logarithm with systematic uncertainties takes on the form:

$$\log L(\vec{E}_{\bar{\nu}_e}|\vec{\eta}) = -N_{exp} + \sum_{i=1}^{N_{events}} \log(f(E_{\bar{\nu}_e}^i|\vec{\eta})) + \frac{1}{2} \sum_{j=1}^{N_{SP}} \frac{\delta\eta_{k_j}^2}{\sigma_j^2} \quad (5)$$

In this work, we used the total of nine continuous parameters. These are four neutrino oscillation parameters: $\sin^2(2\theta_{12})$, $\sin^2(2\theta_{13})$, Δm_{12}^2 , Δm_{13}^2 . Note that for each of the two mass hierarchies, Δm_{23}^2 is determined by the two other squared mass differences and has not to be introduced into the parameter space. Five parameters were dedicated to systematic uncertainties: two geo-neutrino parameters and three detector-associated systematic errors as described in the previous section. The geo-neutrino parameters are left unconstrained, which is equivalent to infinite σ in (4). The default values for the systematic errors in “efficiency”, energy resolution estimation and energy scale were taken to be 2%, 8% and 1%, respectively, which is reasonably conservative for experiments of this kind. Additionally, two extreme cases were analyzed: the most “optimistic” one — with the corresponding parameters fixed at zero deviations as if they were known exactly, and the most “pessimistic” one — with those three uncertainties left unconstrained as well as geo-neutrino parameters. Although practically impossible, these limiting cases indicate how much sensitivity can be gained by improving the systematics and, conversely, how much would be lost if the systematic errors of the real experiment happen to be worse than expected.

“SOLAR” MIXING ANGLE θ_{12}

The “solar” mixing angle has been fairly well constrained by SNO [3] and KamLAND [4]. Our computations suggest that there is still an opportunity for a significant improvement, though.

This measurement is moderately sensitive to detector-based systematic uncertainties but the terrestrial antineutrino background is much more troublesome (Fig 3). These background decrease the sensitivity by about a factor of two and drives the optimum baseline for this parameter to about 60 km, which conflicts with the goal of measuring θ_{13} and Δm_{13}^2 in the same experiment as well. Constraining the geo-neutrino flux would change the situation, but currently there seems to be no way of doing that. The geo-neutrino flux measurements made by KamLAND [4, 26] are not nearly precise enough to improve the situation noticeably and, besides, not directly applicable to a future experiment located elsewhere, especially in the ocean.

Even with that background and the associated uncertainty, the sensitivity of the medium-baseline experiment is noteworthy. For a 10 KT detector at 50 km from a 6 GWt nuclear plant, an exposure of 300 gigawatt-kiloton-years (5 years) is required to achieve the one-sigma confidence range of 0.01 in $\sin^2(2\theta_{12})$, which is about 5 times better than the current best estimation. At 60 km, the same precision can be achieved with just above one-third of this exposure.

Although higher energy resolution is always better, the θ_{12} study does not exhibit appreciable dependence on this parameter and $0.05 \times \sqrt{E_{vis}[MeV]}$ is almost as good as $0.025 \times \sqrt{E_{vis}[MeV]}$. Of the detector-associated systematics, the most significant is the “efficiency” uncertainty.

“SOLAR” SQUARED MASS DIFFERENCE Δm_{12}^2

The measurement of this parameter by KamLAND is more difficult to improve on. For example, the target sensitivity for Hanohano is $0.07 \times 10^{-5} eV^2$, which would be about three times better than the current best estimation. As our calculations suggest, this can be achieved in 300 gigawatt-kiloton-years at the 60 km baseline or in 450 gigawatt-kiloton years from 50 km.

Still longer baselines offer better sensitivity for this particular study (Fig 4) but would be clearly sub-optimal for all other oscillation parameters. The part (b) of the plot shows the dramatic effect of terrestrial neutrino background and, particularly, the uncertainty of this background. Without geo-neutrinos, the same detector would be four times more efficient at 60 km and seven times at 50 km.

The fact that geo-neutrinos drive the optimum baseline towards longer distance may seem somewhat counter-intuitive. The shorter the baseline, the higher the reactor $\bar{\nu}_e$ rate, so the relative fraction of terrestrial $\bar{\nu}_e$ background is smaller and should have a smaller effect. However, at shorter baselines, the reactor $\bar{\nu}_e$ deficit due to oscillations appears mostly in the lower-energy zone where it is harder to separate from the variation in the terrestrial neutrino background.

Like the θ_{12} measurement, this study is not demanding of detector energy resolution and not particularly sensitive to detector-associated systematics.

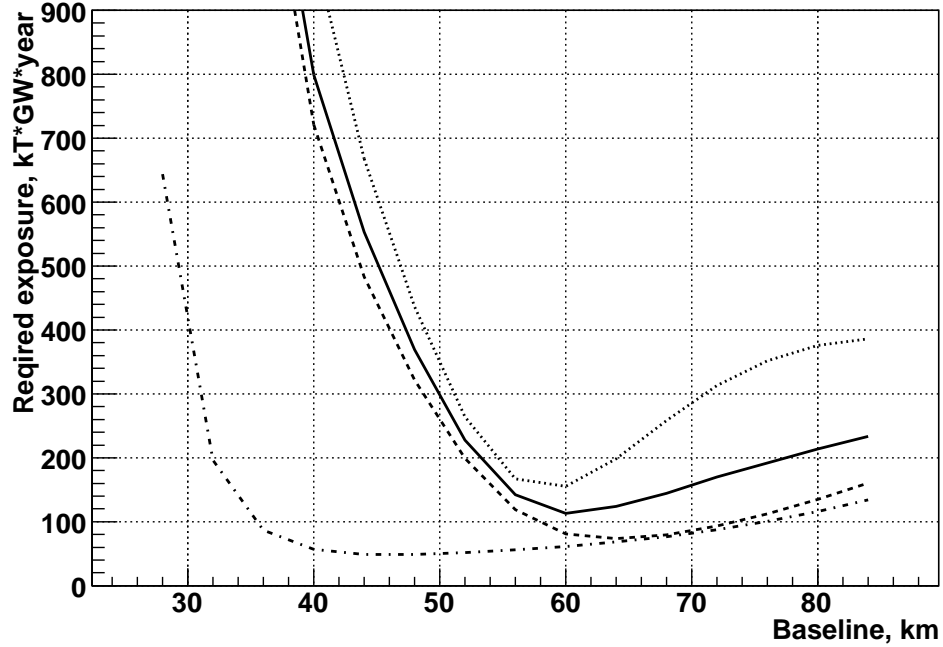


FIG. 3: Exposure yielding the sensitivity of 0.01 in $\sin^2 2\theta_{12}$, as a function of baseline: with unconstrained detector systematics (dotted), with “default” detector systematics (solid), assuming no detector systematics (dashed), assuming no detector systematics and no geo-neutrinos (dot-dashed).

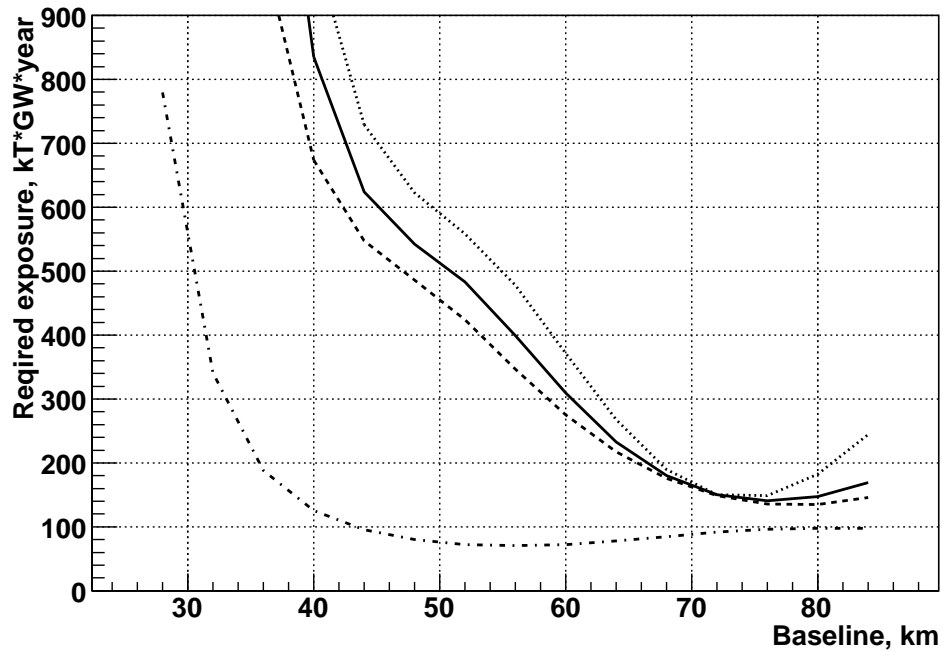


FIG. 4: Exposure yielding the sensitivity of $0.07 \times 10^{-5} eV^2$ in Δm_{12}^2 , as a function of baseline: with unconstrained detector systematics (dotted), with “default” detector systematics (solid), assuming no detector systematics (dashed), assuming no detector systematics and no geo-neutrinos (dot-dashed).

MIXING ANGLE θ_{13}

This is a very important oscillation parameter not only because of its theoretical significance but also because its value defines the amplitude of the sub-dominant high-frequency oscillations governed by Δm_{13} and Δm_{23} . Only if θ_{13} is not zero (and not too small) is it possible to measure those mass squared differences in $\bar{\nu}_e$ disappearance experiments. Currently, only an upper bound for this angle is known (from the CHOOZ experiment [30]): $\sin^2 2\theta < 0.1$. Several experiments are proposed or already under construction to set better limits and the Hanohano detector can contribute to those efforts.

The sensitivity profiles (Figure 5) show that medium baselines (above 30 km) are not optimal for this study and much shorter ones are better from the statistical standpoint. However even at 50 km the absolute sensitivity can be quite impressive with a big detector. Except for the longest baselines (60 km and above) which are clearly sub-optimal, this study is not severely affected by the geo-neutrino background and its uncertainties. The systematics of the detector itself, however, play a more important role here. At 50 km, the main systematic error is the uncertainty of energy resolution estimation, followed by the “efficiency” error. At shorter baselines the “efficiency” uncertainty dominates.

Although the medium baselines have a strong statistical disadvantage for θ_{13} measurement, they also have the compelling feature that systematic uncertainties do not ruin the measurement. Unlike the shorter baseline experiments where relatively more information is obtained through the neutrino event rate, the spectrum shape distortion characteristic of medium baseline is not so easy to imitate by any of the detector systematic errors. This means that, in the long run when even better accuracy for θ_{13} is required, medium baseline experiments may prove to be more robust.

Figure 6 exhibits another important feature of this measurement: its energy resolution dependence. Although not as critical as for the hierarchy study (below), the effect of detector energy resolution is quite noticeable. Compromising this parameter to $0.05 \times \sqrt{E_{vis}[MeV]}$ from the $0.025 \times \sqrt{E_{vis}[MeV]}$ (as projected for Hanohano) will cost about 2.5 times the exposure.

Δm_{13}^2 AND Δm_{23}^2

Unlike all previously considered parameters where the potential sensitivity of an experiment could be predicted more or less accurately based just on the $\bar{\nu}_e$ exposure, this measurement depends on the value of θ_{13} which is still unknown. Any quantitative sensitivity prediction makes sense only with some particular value of θ_{13} in mind. The larger the mixing angle, the easier it is to determine Δm_{13}^2 , Δm_{23}^2 and neutrino mass hierarchy. It has been found that the sensitivity scales approximately as the square of $\sin^2 2\theta_{13}$. In other words, getting the same sensitivity in Δm_{13}^2 , Δm_{23}^2 and neutrino mass hierarchy if $\sin^2 2\theta_{13} = 0.01$ will take four times the exposure required if $\sin^2 2\theta_{13} = 0.02$. In this paper we carried out calculations for two scenarios: $\sin^2 2\theta_{13} = 0.05$, and $\sin^2 2\theta_{13} = 0.025$.

Another ambiguity associated with the study of Δm_{13}^2 and Δm_{23}^2 follows from the closely related question of neutrino mass hierarchy. Depending on the actual value of the mixing angle θ_{13} , the neutrino mass hierarchy may turn out unfeasible to establish at an adequate CL. At the same time, within each of the two possible hierarchies, stringent limits on both Δm_{13}^2 and Δm_{23}^2 may still be set with reasonable exposures. Since the ambiguity is at worst only a two-fold one, it makes sense to estimate the “known-hierarchy” sensitivity to either Δm_{13}^2 or Δm_{23}^2 .

Figure 7 and 8 show that shorter baselines are better for this study, although this trend is not as pronounced as with θ_{13} measurement and actually reverses below 25 km. It is clear that Δm_{13}^2 study is not systematics-constrained, including the systematics from geo-neutrinos. On the other hand, the dependence on energy resolution for this measurement is even stronger than that for θ_{13} (Figure 9 and 10).

NEUTRINO MASS HIERARCHY

Like the $\Delta m_{13}^2/\Delta m_{23}^2$ measurement, the hierarchy study depends on the actual value of θ_{13} . Our calculations suggest that for any θ_{13} it takes more statistics to make a high confidence level conclusion about the hierarchy than to measure Δm_{13}^2 and Δm_{23}^2 to an accuracy of $0.025 \times 10^{-3} eV^2$. This makes reliable hierarchy determination with a 10 kt detector feasible only if the mixing angle turns out to be quite high ($\sin^2 2\theta_{12} \geq 0.05$). The sensitivity dependence on this value is approximately quadratic in the exposure as well. The baseline profile of the sensitivity to the hierarchy is shown in Figure 11. After taking into account the geo-neutrino background and the uncertainties the optimum baseline remains in the same range as was found earlier with less comprehensive models [8, 27] — 50 km or slightly

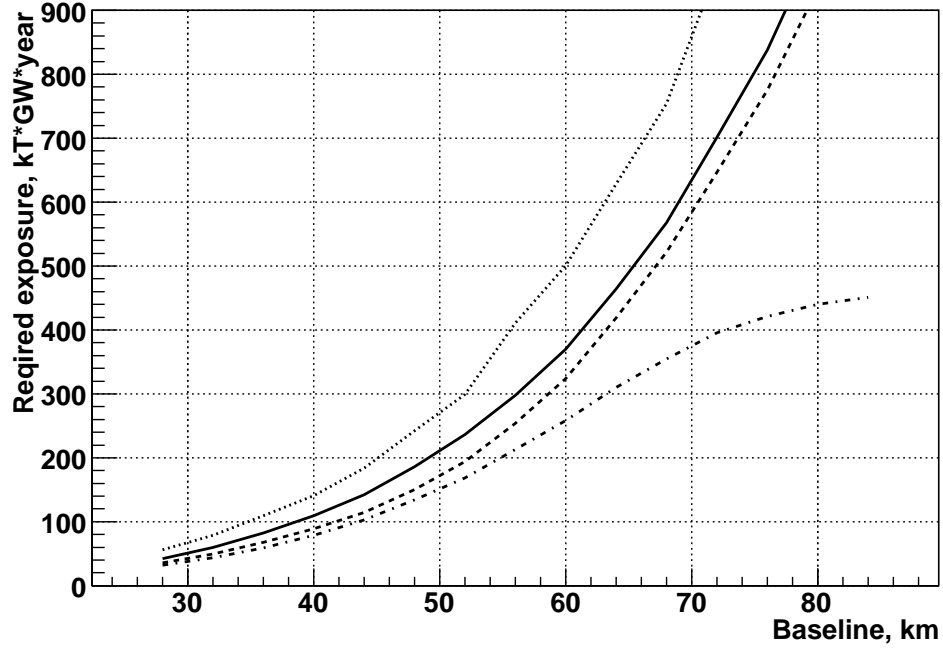


FIG. 5: Exposure yielding the sensitivity of 0.02 in $\sin^2 2\theta_{13}$, as a function of baseline: with unconstrained detector systematics (dotted), with “default” detector systematics (solid), assuming no detector systematics (dashed), assuming no detector systematics and no geo-neutrinos (dot-dashed). Detector energy resolution equal to $0.025 \times \sqrt{E_{vis}[\text{MeV}]}$ is assumed.

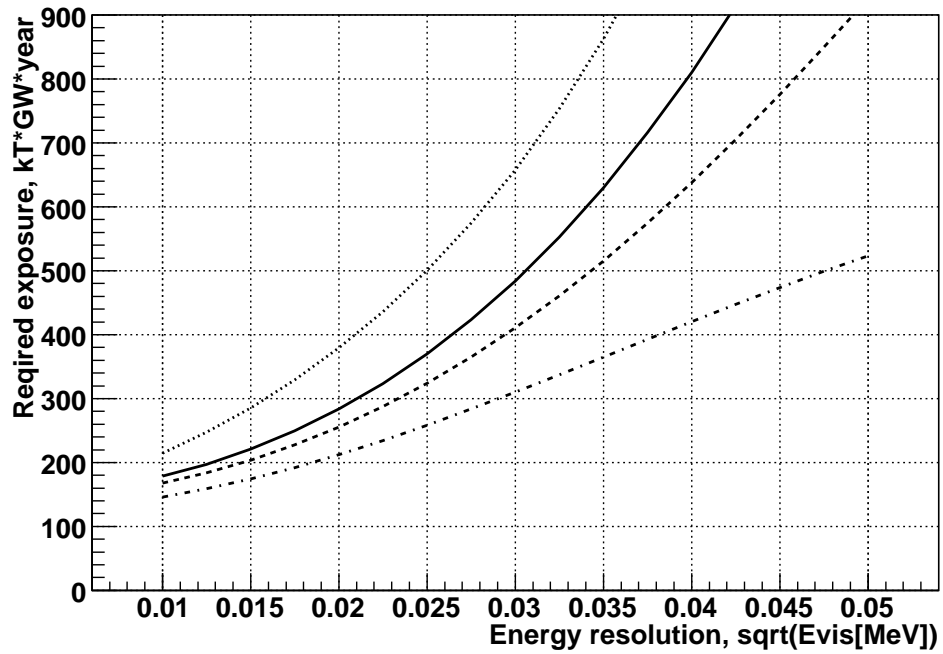


FIG. 6: Exposure yielding the sensitivity of 0.02 in $\sin^2 2\theta_{13}$ from the baseline of 60 km, as a function of the detector energy resolution: with unconstrained detector systematics (dotted), with “default” detector systematics (solid), assuming no detector systematics (dashed), assuming no detector systematics and no geo-neutrinos (dot-dashed).

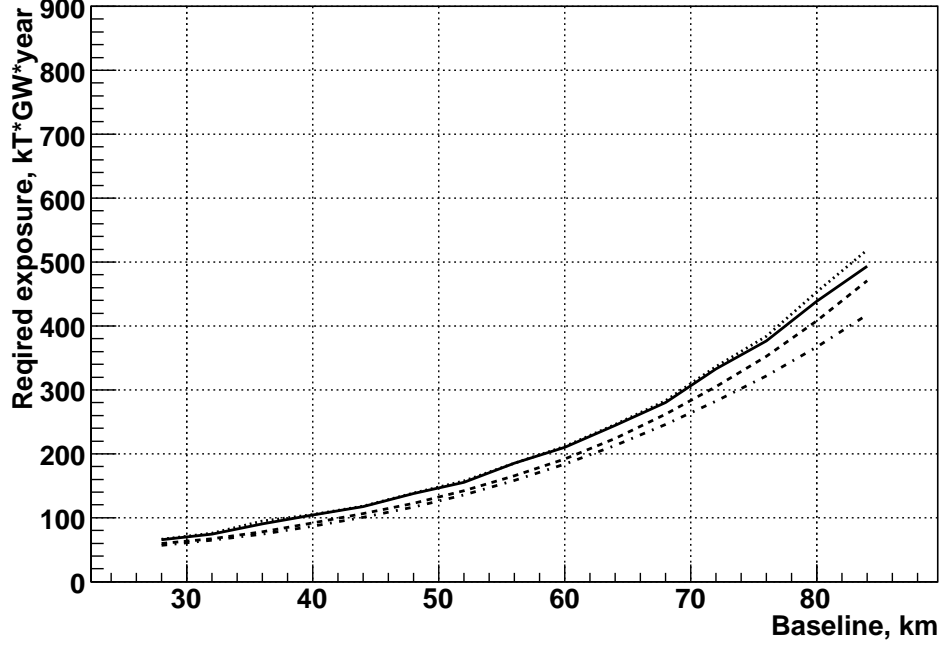


FIG. 7: Assuming $\sin^2 2\theta_{13} = 0.05$: exposure yielding the sensitivity of $0.025 \times 10^{-3} eV^2$ in Δm_{13}^2 within a given mass hierarchy, as a function of baseline: with unconstrained detector systematics (dotted), with “default” detector systematics (solid), assuming no detector systematics (dashed), assuming no detector systematics and no geo-neutrinos (dot-dashed). Detector energy resolution equal to $0.025 \times \sqrt{E_{vis}[MeV]}$ is assumed.

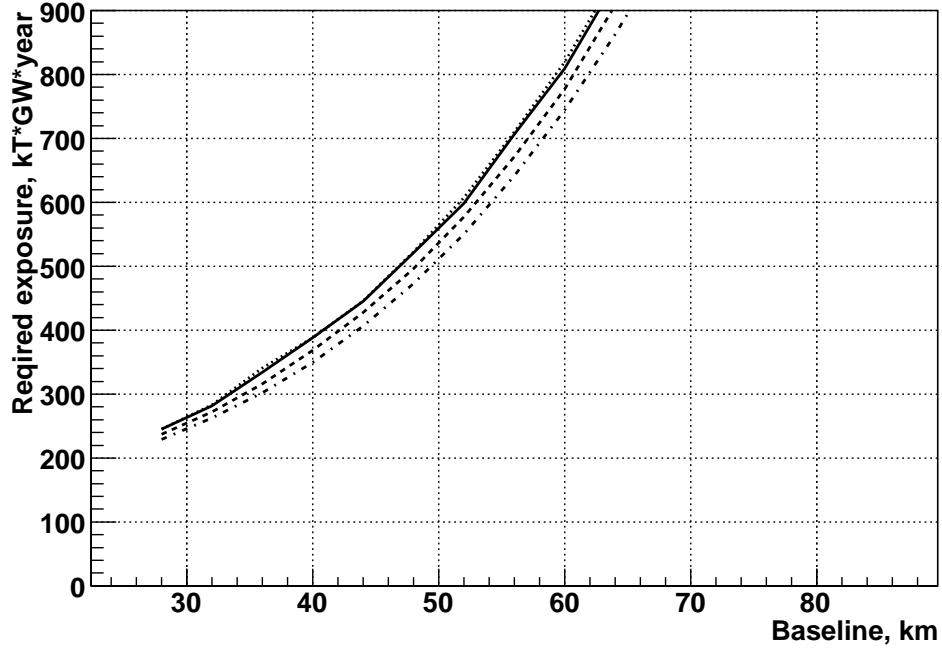


FIG. 8: Assuming $\sin^2 2\theta_{13} = 0.025$: exposure yielding the sensitivity of $0.025 \times 10^{-3} eV^2$ in Δm_{13}^2 within a given mass hierarchy, as a function of the baseline: with unconstrained detector systematics (dotted), with “default” detector systematics (solid), assuming no detector systematics (dashed), assuming no detector systematics and no geo-neutrinos (dot-dashed). Detector energy resolution equal to $0.025 \times \sqrt{E_{vis}[MeV]}$ is assumed.

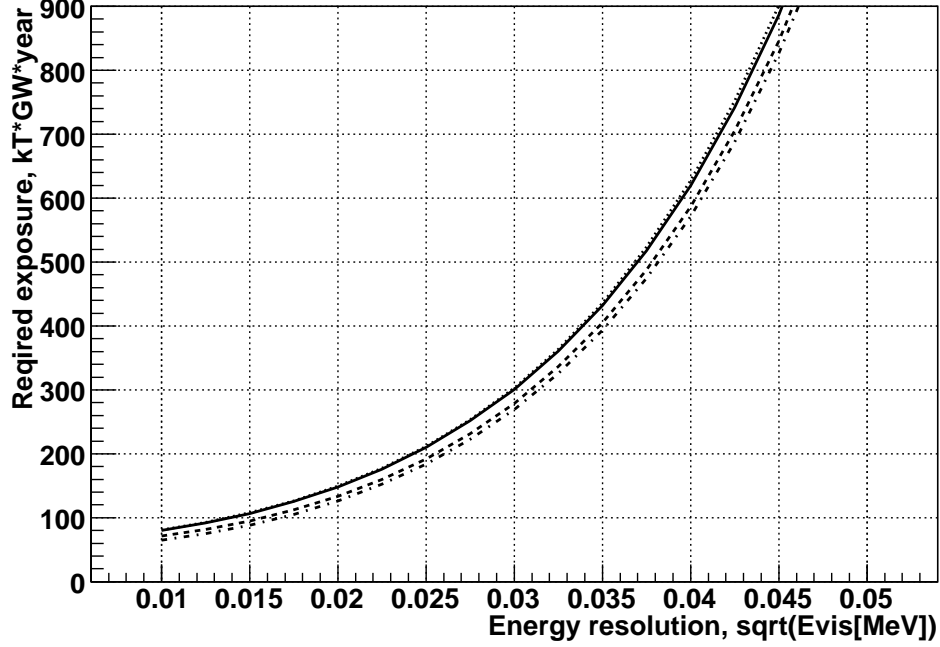


FIG. 9: Assuming $\sin^2 2\theta_{13} = 0.05$: exposure yielding the sensitivity of $0.025 \times 10^{-3} eV^2$ in Δm_{13}^2 within a given mass hierarchy, as a function of detector energy resolution: with unconstrained detector systematics (dotted), with “default” detector systematics (solid), assuming no detector systematics (dashed), assuming no detector systematics and no geo-neutrinos (dot-dashed). 60 km baseline is assumed.

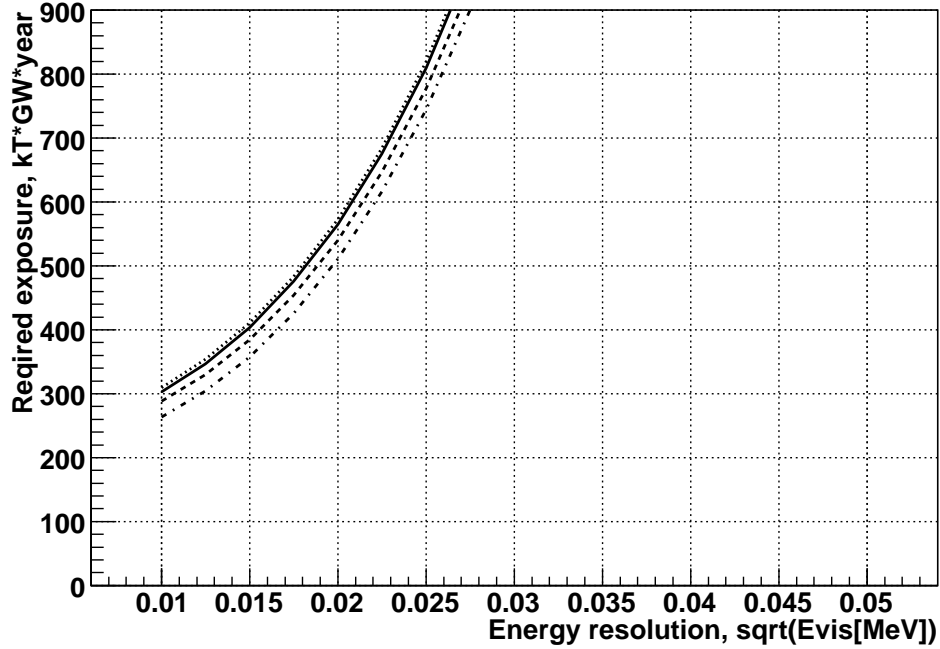


FIG. 10: Assuming $\sin^2 2\theta_{13} = 0.025$: exposure yielding the sensitivity of $0.025 \times 10^{-3} eV^2$ in Δm_{13}^2 within a given mass hierarchy, as a function of detector energy resolution: with unconstrained detector systematics (dotted), with “default” detector systematics (solid), assuming no detector systematics (dashed), assuming no detector systematics and no geo-neutrinos (dot-dashed). 60 km baseline is assumed.

more. Of the systematic errors, the most damaging is the geo-neutrino flux uncertainty, although its effect is not as decisive as for the solar parameter studies.

The hierarchy study proves to be the most demanding of the detector energy resolution (Figure 12). Even within the best values for that parameter of the detector achievable today the sensitivity dependence on the energy resolution enters its asymptotic 4-th power curve. In particular, this implies that between two detectors of the same photocathode area but different volumes, the bigger detector will offer *inferior* sensitivity: all other parameters being equal, a smaller relative photocathode coverage will lead to lower resolution which will prevail over the higher reactor $\bar{\nu}_e$ statistics.

Theoretically, the mass hierarchy study is secondary to the measurement of Δm_{13}^2 and Δm_{23}^2 and is determined immediately after those mass differences are found. The analysis of the oscillated $\bar{\nu}_e$ energy spectrum yields all mass differences (provided, $\theta_{13} \neq 0$ and $\theta_{12} \neq \pi/4$). In practice, however, the squared mass differences can be measured with limited accuracy only and at a limited CL. This may not be sufficient to determine the hierarchy. Moreover, it has been found [35] that for any combination of Δm_{13}^2 and Δm_{23}^2 there exists another one (denoted below as $\Delta' m_{13}^2$ and $\Delta' m_{23}^2$) that delivers a similar oscillation pattern despite comprising the opposite mass hierarchy. The similarity is never perfect and, given enough statistics, it is always possible to distinguish between the two spectra but it may take much more exposure to discriminate between those “conjugate” opposite hierarchy solutions than to constrain the squared mass differences within one of the solutions with a remarkable precision.

In Figure 13, the curves provide the measure of relative “unlikeliness” of an alternative hypothesis, assuming normal hierarchy and $\Delta m_{13}^2 = 2.4 \times 10^{-3} eV^2$, for which the experiment was simulated. Zero χ^2 means an indistinguishable hypothesis, the higher its value, the less statistics is needed to discriminate the hypothesis. Solid lines show the normal hierarchy and dotted lines show the inverted one. The dashed vertical lines through the centers of the dotted curves point to the $\Delta' m_{13}^2$ which combined with the inverted hierarchy provide the closest similarity to the simulated physical spectrum. Comparison of Figure 13(a) and Figure 13(b) explains why the 60 km baseline offers better hierarchy discrimination than 40 km, although the latter yields significantly better sensitivity to $\Delta m_{13}^2/\Delta m_{23}^2$ within each of the two hierarchies: the vertex of the quasi-parabolic dotted curve is located higher for 60 km.

The “conjugate” $\Delta' m_{13}^2$ for a given real Δm_{13}^2 is not the same for different baselines, which implies that two measurements at different baselines may offer improved efficiency. For instance, the allowable values of $\Delta' m_{13}^2$ to which the 60 km baselined measurement is least sensitive are much better excluded at 40 km and vice versa. In case of a land-based detection, a multiple-detector configuration can be considered. Hanohano, additionally, can use the advantage of its movability and make two consecutive exposures instead of one twice as long. Indeed, as the comparison between Figure 13(c) and Figure 13(d) shows, the combination of 60 and 40 km baselined observations should provide a better hierarchy resolution than one twice as long at the practically optimal 50 km. Although the advantage is marginal, we considered only a two-baseline combination with equal exposures. A more systematic optimization with different exposures and possibly more than just two baselines should offer further gains.

CONCLUSION

With a single detector and a 300 kiloton-gigawatt-year exposure and a 5-6 GW thermal power $\bar{\nu}_e$ source, both Δm_{12}^2 and θ_{12} are expected to be measured with the accuracy of 1%, a three to five time improvement on the current best limits [4]. An experiment with a more powerful reactor $\bar{\nu}_e$ source but the same exposure due to a smaller detector size or a shorter livetime will have a slight advantage because of the relatively smaller geo-neutrino effect.

Detector-associated systematic uncertainties do not appear to be a significant limiting factor in the resulting accuracy. These studies are not particularly sensitive to the detector resolution and $5 - 6\% \times \sqrt{E_{vis} [MeV]}$ would be quite sufficient. However the expected sensitivity, especially that for Δm_{12}^2 , will be severely handicapped by the presence of geo-neutrinos and in particular by the lack of accurate estimation for the intensity of this background source, effectively turning its value into yet another systematic uncertainty — the dominating one for this study. This is not a “hard” limitation since geo-neutrinos, having a different spectrum, can not mimic the reactor $\bar{\nu}_e$ oscillation pattern, but rather an efficiency impairment.

The study of the θ_{13} mixing angle is different, in that the medium baselines that this study deals with are not optimal. On a per-event basis, the baseline dependence of sensitivity is rather flat, but short baselines gives quadratically higher event rate and hence lower statistical error. On the other hand, longer baselines offer more robustness with respect

[35] This problem had been pointed to in [23] and [32]. Our simulations confirm it, no matter whether Fourier transform is used in the data analysis or not.

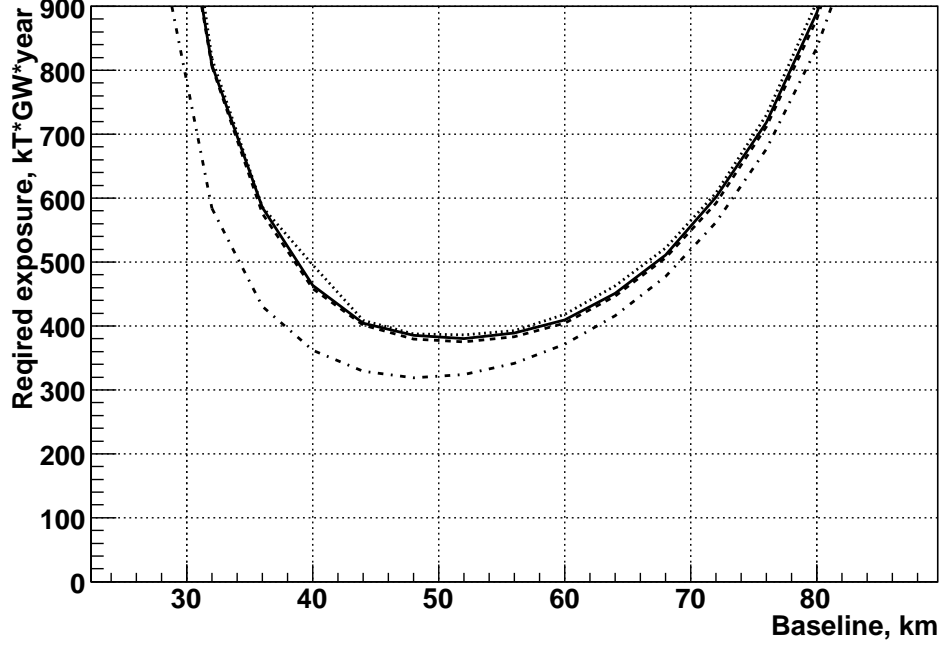


FIG. 11: Assuming $\sin^2 2\theta_{13} = 0.05$: exposure necessary to discriminate the neutrino mass hierarchies to 66.8% CL, as a function of baseline: with unconstrained detector systematics (dotted), with “default” detector systematics (solid), assuming no detector systematics (dashed), assuming no detector systematics and no geo-neutrinos (dot-dashed). Detector energy resolution equal to $0.025 \times \sqrt{E_{vis}[\text{MeV}]}$ is assumed.

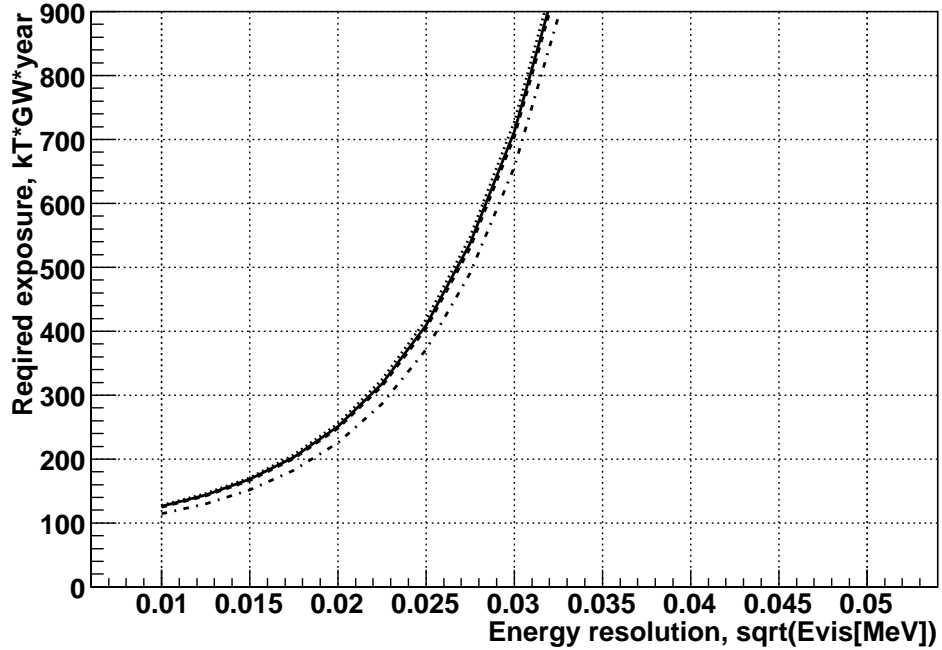


FIG. 12: Assuming $\sin^2 2\theta_{13} = 0.05$: exposure necessary to discriminate the neutrino mass hierarchies to 66.8% CL, as a function of detector energy resolution: with unconstrained detector systematics (dotted), with “default” detector systematics (solid), assuming no detector systematics (dashed), assuming no detector systematics and no geo-neutrinos (dot-dashed). 60 km baseline is assumed.

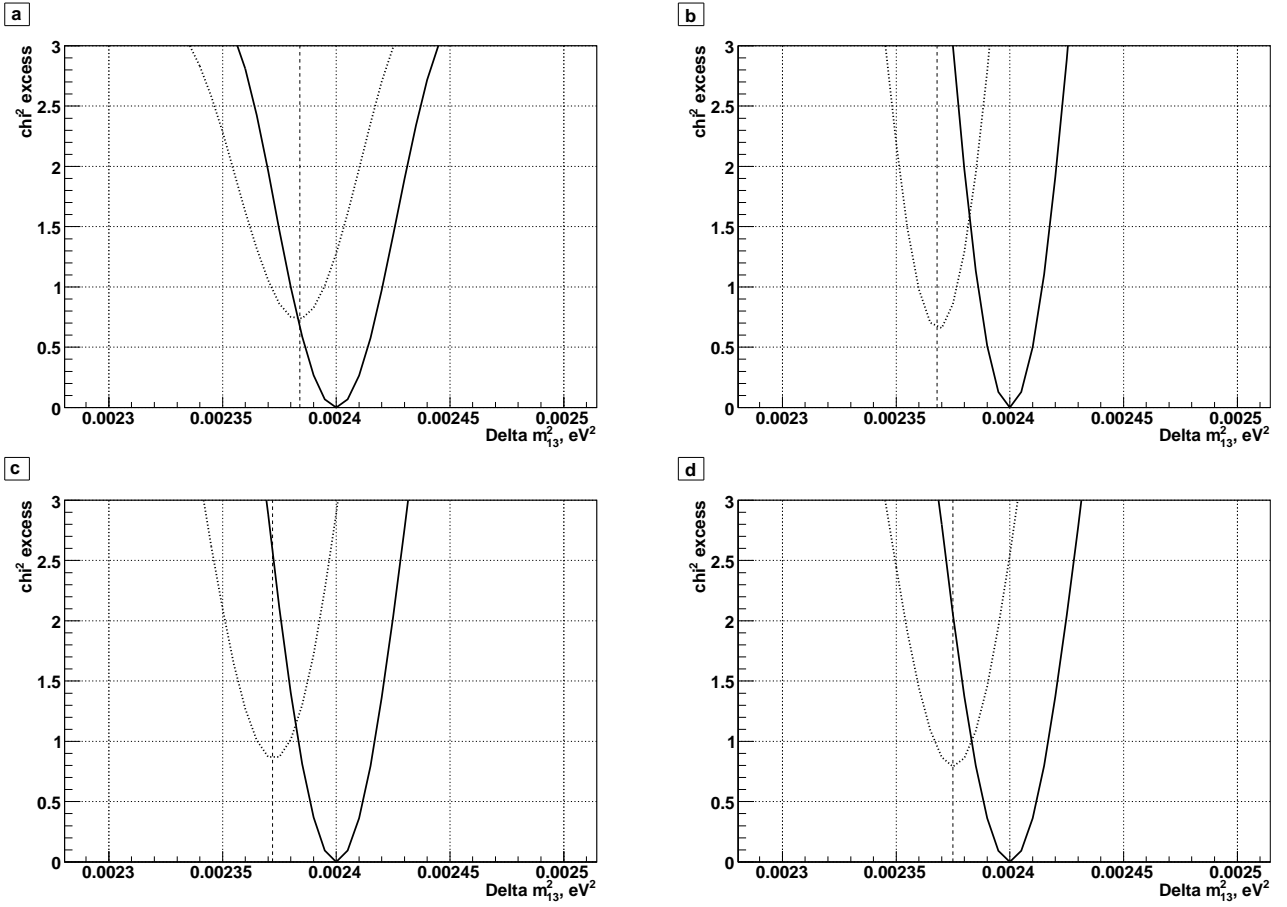


FIG. 13: χ^2 excess for an alternative hypothesis about the Δm_{13}^2 and the mass hierarchy over the “real” one for which the events were simulated ($\Delta m_{13}^2 = 2.4 \times 10^{-3} eV^2$, normal hierarchy). Solid line is for “correct” hierarchy, dotted – for the “wrong” one. The larger the χ^2 excess, the easier the alternative hypothesis to rule out. (a) single detector at 60 km; (b) single detector at 40 km; (c) two half-sized detectors, one at 60 km and another at 40 km; (d) single detector at 50 km.

to the “efficiency” systematic uncertainty. Given the careful design of Hanohano or any similar (considering the size and the baseline) detector and its accurate calibration, it is still possible to reach an accuracy of better than 0.02 in $\sin^2 2\theta_{13}$ evaluation, which is competitive with the dedicated experiments like Double Chooz and Daya Bay. The sensitivity to this mixing angle does not exhibit strong dependence on its own real value. In other words, setting the upper limit of 0.02 for $\sin^2 2\theta_{13}$ if the angle happens to be zero takes about as much exposure as setting the range between 0.03 and 0.07 if the value is really 0.05.

The measurement of Δm_{13}^2 and Δm_{23}^2 and the closely related question of neutrino mass hierarchy are common in their dependence on the actual value of θ_{13} . If the angle turns out to be big enough (within currently allowed values), then some spectacular results are possible. If it is zero or very small, nothing interesting can be measured with either Hanohano or any other similar experiment. The necessary exposure is approximately inversely quadratic to the value of $\sin^2 2\theta_{13}$ in both cases, although the hierarchy measurement generally requires much more statistics. For a moderately optimistic scenario in which $\theta_{13} = 0.025$, Hanohano or a similar experiment can yield a very good estimation for the values of the squared mass differences but reliable mass hierarchy separation may call for prohibitively long exposures. Another feature that these measurements have in common is the requirement for the excellent energy resolution.

Generally, assuming either normal or inverted hierarchy, the problem of Δm_{13}^2 and Δm_{23}^2 becomes simpler, less demanding of the energy resolution and with higher chance of success for unfavorably small values of θ_{13} . Even if the hierarchy question is not conclusively answered at that stage, the squared mass differences can still be measured, even though the remaining hierarchy ambiguity will split the allowable solutions into two groups. In such a case, the result of the Δm_{13}^2 and Δm_{23}^2 study will have the form:

$$\Delta m_{13}^2 = \Delta_{norm} \pm \Delta\delta_{norm}$$

$$\Delta m_{23}^2 = \Delta_{norm} - \Delta m_{12}^2 \pm \Delta\delta_{norm}$$

for normal hierarchy, and

$$\Delta m_{13}^2 = \Delta_{inv} \pm \Delta\delta_{inv}$$

$$\Delta m_{23}^2 = \Delta_{inv} + \Delta m_{12}^2 \pm \Delta\delta_{inv}$$

for inverted hierarchy, with one solution somewhat more favored over the other (i.e. should the hierarchy discrimination be achieved to marginal confidence levels). Here Δ_{norm} and Δ_{inv} are best fit values for the Δm_{13}^2 for the normal and inverted scenarios, respectively, the Δm_{12}^2 is expected to be found from the same experiment with superior accuracy and $\Delta\delta_{norm}$ and $\Delta\delta_{inv}$ are the error bars for both the Δm_{13}^2 and Δm_{23}^2 in the normal and inverted hierarchy, respectively.

The sensitivity properties for oscillation parameters in a single-baseline experiment are summarized in Table I and II.

TABLE I: Parameter sensitivity properties for θ_{12} , Δm_{12}^2 and θ_{13} with Hanohano or similar detectors.

Parameter	θ_{12}	Δm_{12}^2	θ_{13}
Detector systematics dependence	low	low	high
Geo $\bar{\nu}_e$ dependence	high	high	low
$\bar{\nu}_e$ energy resolution dependence	low	low	high
Optimal baseline for single detector, km	60-70	70-80	<20
Expected sensitivity	0.01	$0.07 \times 10^{-5} eV^2$	0.02

As was proposed in [33] and discussed in numerous later publications, neutrinos may have non-standard interactions which could affect the flavor content at the source and also the flavor content detected. For our case at hand, it means that the observed mixing angles θ_{12} and θ_{13} in general will differ from the “true” mixing angles. For example, the measured θ_{13} can be larger than the true θ_{13} [34]. Since the survival probability (2) depends on the effective θ_{13} , the

TABLE II: Sensitivity properties for Δm_{13}^2 (or Δm_{23}^2) and neutrino mass hierarchy.

Parameter	Δm_{13}^2	M. H.
Detector systematics dependence	low	low
Geo $\bar{\nu}_e$ dependence	low	avg
$\bar{\nu}_e$ energy resolution dependence	v. high	extreme
Dependence on θ_{13}	yes	yes
Optimal baseline for single detector, km	<30	50

NSI have no adverse effect on the determination of Δm_{13}^2 , Δm_{23}^2 and the neutrino mass hierarchy. In fact an effective θ_{13} larger than the real one will be advantageous for these studies.

At the same time, the effective θ_{13} measured at different baselines are going to be different, should these interactions take place. This way, medium baseline experiments targeting θ_{13} will become complementary to the short baseline ones in testing new physics.

The two most important qualitative conclusions from this study are the following:

- Medium-baselined $\bar{\nu}_e$ oscillation experiments are not systematics-constrained. This follows from the shapes of oscillated spectra. In particular, physically feasible systematic errors do not tend to imitate the spectral distortions characteristic of the neutrino oscillations.
- There is no single baseline optimal for all oscillation studies. The difference in sensitivity profiles is big enough to give an advantage to multiple detector or/and movable detector configurations. Even in individual studies where a pronounced baseline optimum exists, a multiple baseline configuration can outperform a single baseline configuration, as has been shown for the neutrino mass hierarchy discrimination case.

This work was partially supported by the U.S. Department of Energy grant DE-FG02-04ER41291 and the University of Hawaii.

* Email: batygov@phys.hawaii.edu

† Email: sdye@hpu.edu

‡ Email: jgl@phys.hawaii.edu

§ Email: shige@phys.hawaii.edu

¶ Email: pakvasa@phys.hawaii.edu

** Email: varner@phys.hawaii.edu

- [1] B. Pontecorvo, Sov. Phys. JETP **7**, 172 (1959).
- [2] Z. Maki, M. Nakagawa and S. Sakata, Prog. Theor. Phys. **28**, 870 (1962).
- [3] B. Aharmim *et al.*, Phys. Rev. **C72** 055502 (2005).
- [4] S. Abe, *et al.*, Phys. Rev. Lett. **100**, 221803 (2008).
- [5] F. Reines and C. L. Cowan, Jr., Phys. Rev. **92**, 830 (1953).
- [6] R. Davis, Jr., *et al.*, Phys. Rev. Lett. **20**, 1205 (1968).
- [7] S.T. Dye *et al.*, Earth, Moon, and Planets **99** (2006) 241-252.
- [8] J. G. Learned, S. T. Dye, S. Pakvasa in *Twelfth International Workshop on Neutrino Telescopes*, ed. Baldo Ceolin (Istituto Veneto di Scienze, Padova), p 235 (2007).
- [9] L. Wolfenstein, Phys. Rev. D **17**, 2369 (1978).
- [10] S. P. Mikheev and A. Yu. Smirnov, Sov. J. Nucl. Phys. **42**, 913 (1985).
- [11] H. Schlattl, Phys. Rev. **D64**, 013009 (2001).
- [12] S. M. Bilenky, D. Nicole and S. T. Petcov, Phys. Lett. **B538** (2002) 77-86.
- [13] Q. R. Ahmad, *et al.*, Phys. Rev. Lett. **89** 011301 (2002).
- [14] S. Fukuda *et al.*, Phys. Lett. **B539** (2002) 179-187.
- [15] M. Ishitsuka, for the Super-Kamiokande Collaboration, hep-ex/0406076 (2004).
- [16] M. H. Ahn, *et al.*, Phys. Rev. **D74**, 072003 (2006).
- [17] P. Adamson *et al.* (MINOS), Phys. Rev. **D73** (2006) 072002.
- [18] G. L. Fogli, *et al.*, Phys. Rev. Lett. **101** 141801 (2008).
- [19] K. Shreckenbach *et al.*, Phys. Lett. **B160** 325 (1985).
- [20] P. Vogel *et al.*, Phys. Rev. **C24** 1543 (1981).

- [21] P. Vogel, J. F. Beacom, Phys. Rev. D **60**, 053003 (1999).
- [22] S. T. Petcov and M. Piai, Phys. Lett B. **533**, 94 (2002) arXiv:hep-ph/0112074.
- [23] S. Choubey, S. T. Petcov, M. Piai, Phys. Rev. D **68**, 113006 (2003) arXiv:hep-ph/0306017v1.
- [24] A. Bandyopadhyay, S. Choubey, S. Goswami, S.T. Petcov, D.P. Roy, (2008) arXiv:0804.4857v1 [hep-ph]
- [25] M. Balata, *et al.*, Eur.Phys.J. **C47** (2006) 21-30.
- [26] T. Araki *et al.*, , Nature **436**, 499 (2005).
- [27] J. G. Learned, S. T. Dye, S. Pakvasa, R. C. Svoboda, hep-ex/0612022, Phys. Rev. D (in press).
- [28] K. Eguchi *et al.*, Phys. Rev. Lett. **90**, 021802 (2003).
- [29] T. Araki *et al.*, Phys. Rev. Lett. **94**, 081801 (2005).
- [30] M. Apollonio *et al.*, Eur. Phys. J. C **27**, 331 (2003).
- [31] Glen Cowan, "Statistical Data Analysis", Oxford Science Publications, 1998.
- [32] Stephen Parke, private communication.
- [33] Y. Grossman, Phys Lett **B359** (1995) 141.
- [34] T. Ohlsson and H. Zhang, arXiv:0809.4835 (2008) [hep-ph].